Renewable Energy 253 (2025) 123597

Contents lists available at ScienceDirect

Renewable Energy

journal homepage: www.elsevier.com/locate/renene

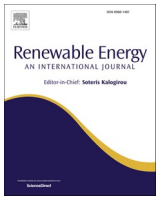

Technoeconomic feasibility of a waste-to-energy (WtE) polygeneration system implementing circular carbon strategies: A case study for Spain

Farzin Ahmadi [a,*], Reza Shirmohammadi [b], Fèlix Llovell [b], Majid Amidpour [c]

[a] Department of Energy and Mechanical Engineering, School of Engineering, Aalto University, FI-00076, Espoo, Finland
[b] Department of Chemical Engineering, ETSEQ, Universitat Rovira i Virgili, Avda Països Catalans 26, 43007, Tarragona, Spain
[c] Department of Energy System Engineering, Faculty of Mechanical Engineering, K. N. Toosi University of Technology, Tehran, 11365-4435, Iran

ARTICLE INFO

Keywords:
Waste to energy
Technoeconomic
Carbon capture and utilization
Hydrogen
Methanol
Freshwater

ABSTRACT

Waste-to-energy (WtE) polygeneration systems present an integrated solution for addressing waste management challenges, while in parallel producing energy, fuels, and freshwater. In this paper, a new WtE system based on wood residues is proposed. The system consists of an integrated biomass gasification combined cycle including carbon capture, hydrogen separation, methanol synthesis, multi-stage flash desalination, and domestic heating systems. Hydrogen can be used directly as a fuel or an intermediate product. The captured carbon is utilized for methanol production, which enhances system flexibility and overall performance. A technoeconomic analysis is carried out using total revenue requirement (TRR) method to assess the feasibility of the system. In addition, a parametric study is conducted, evaluating the system from energy and exergy perspectives based on key indicators. Besides, a genetic optimization algorithm is employed to determine the optimum for various cases to maximize power generation, enhance efficiencies, and promote sustainability. The energy and exergy efficiencies for the base case are 55.22 % and 37.92 %, which are improved up to 67.58 % and 46.64 % after exergy optimization. The LCOE and LCOH, for the benchmark system, obtained as 0.08 $/kWh and 0.04 $/kWh, while the $LCOH_2$, LCOM, and LCOW are 2.43 $/kg, 0.33 $/kg, and 0.12 $/$m^3$, respectively.

1. Introduction

Nowadays, human life remains heavily dependent on fossil fuels for essential needs such as heating, electricity generation, and transportation. This over-reliance on conventional fossil fuels not only depletes finite natural resources, but also significantly contributes to environmental pollution, global warming and climate change [1]. As these environmental challenges intensify, there is an urgent need for sustainable alternatives that can mitigate the impacts of fossil fuel use [2]. In response, various forms of renewable energy have been explored, with the advancement of these technologies becoming increasingly essential [3]. Harnessing renewable energy sources such as biomass, geothermal, solar, wind, and hydro offers the potential to reduce pollutant emissions and further slow down the depletion of fossil fuels, making them an appealing alternative. Their utilization is also believed to promote sustainable development [4]. This approach enhances the performance of conventional energy systems with environmental advantages.

Among renewable sources, one promising solution lies in waste-to-energy (WtE) technologies, offering the dual benefit of reducing waste volumes and generating renewable energy [5]. WtE processes convert municipal solid waste, agricultural residues, and industrial by-products into electricity, heat, or fuels [6]. This not only helps in diverting waste from landfills, reducing methane emissions, but also lessens the demand for fossil fuels by providing a renewable energy source [7]. The integration of WtE systems can contribute to the circular economy by turning waste into a valuable resource, lowering greenhouse gas emissions, and enhancing energy security. By efficiently utilizing waste, WtE technologies provide a cleaner and more sustainable energy solution for the future, making them an essential component of the efforts to reduce environmental degradation and promote sustainable development [8].

At a global level, WtE is widely recognized as a sustainable strategy for addressing waste management and energy generation challenges, as it limits greenhouse gas emissions and land consumption while producing useful energy [9]. Many countries have deployed various WtE technologies – such as incineration, gasification, pyrolysis, and anaerobic digestion – to convert waste into electricity, heat, and fuels [10]. Among these approaches, gasification can convert heterogeneous

* Corresponding author.
E-mail address: Farzin.ahmadi@aalto.fi (F. Ahmadi).

https://doi.org/10.1016/j.renene.2025.123597
Received 12 December 2024; Received in revised form 30 April 2025; Accepted 29 May 2025
Available online 30 May 2025

feedstocks into syngas suitable for the production of electricity, heat, or fuels, although certain thermochemical processes can be cost-intensive due to the high temperatures required [11,12]. Nevertheless, biomass gasification is widely recommended in the literature as an efficient method to produce clean energy and value-added chemicals [12–14]. Meanwhile, international interest in WtE continues to grow amid rising waste generation and resource depletion concerns. Notably, worldwide municipal solid waste production is projected to increase from about 2.01 billion tonnes in 2016 to 3.40 billion tonnes by 2050 [15], clearly showing the urgency of implementing efficient WtE systems. To evaluate the viability of such systems, numerous technoeconomic feasibility studies have been conducted. For instance, a recent analysis in Colombia showed that WtE projects can achieve internal rates of return above 10 % (reaching roughly 14 % in some cases) when supported by appropriate policies and incentives [16]. These findings highlight that, under favorable conditions, WtE facilities can provide both environmental benefits and economic profitability as part of an integrated waste management strategy.

In line with these benefits, WtE adoption has been rising worldwide, as it reduces reliance on landfills and lowers greenhouse gas emissions. Developed countries have incorporated WtE into their waste management strategies—for example, China incinerated about 19 % of its municipal waste in 2010 and Japan operates around 1900 incineration plants [16]. In developing regions, incineration-based WtE is often seen as a reliable and economical waste treatment solution [16]. Consequently, numerous technoeconomic studies have evaluated the feasibility of WtE systems under various scenarios. These analyses reveal that project viability strongly depends on feedstock characteristics and is significantly enhanced by supportive policies and incentives [16,17]. Nevertheless, there remain gaps in understanding the large-scale implementation of WtE systems—such as feedstock heterogeneity, effective policy mechanisms, and integration with other renewables—that, once optimized, can further strengthen their economic viability and environmental benefits.

While various renewable sources are integrated into energy conversion systems, each with its own set of advantages and drawbacks, biomass stands out as a highly valuable renewable resource, particularly in regions with abundant forests. For example, agricultural byproducts such as livestock manure, crop residues (e.g., bagasse and wheat straw), and forest waste are promising biomass feedstocks in Spain [18], which can be converted using well-established thermochemical and biochemical processes [19]. In particular, Spain has the potential to produce up to 163 TWh of bioenergy per year, though this capacity varies significantly across regions due to factors such as climate conditions, land availability, agricultural and forestry practices. These approximations can be boosted by thermal gasification making a total of 190 TWh [18]. A second study only focused in biomethane production reported a potential of 137 TWh [20]. For success, each process should be selected based on available infrastructure and specific objectives.

Among different configurations, polygeneration systems are becoming more prevalent in sustainable energy strategies due to their ability to produce multiple outputs, including power and thermal energy, and their capacity to better utilize excess heat that would be wasted in conventional energy systems. Moreover, these systems have a wide range of applications, including utilities, buildings, sectors, and different industrial clusters, such as pulp, plastic, agriculture, and chemical [21–23]. Numerous studies have investigated a variety of polygeneration systems [24–26], emphasizing the growing attention towards developing clean, flexible, and efficient energy solutions. By simultaneously producing multiple energy carriers, these systems aim to maximize resource utilization, reduce waste, and enhance sustainability.

In this regard, Neri et al. [27] modeled a network for urban-industrial symbiosis that combines anaerobic digestion, cogeneration, photovoltaic, and hydrogen technologies. The model, exemplified in Emilia-Romagna (Italy), enhances site selection based on economic, environmental, and social factors, boosting energy and hydrogen production, while reducing carbon footprint and creating job opportunities. Similarly, Pang et al. [28] elaborated on incorporation of hydrogen into urban and industrial energy systems. An optimal distribution of power, cooling, heating, and hydrogen energy is achieved by formulating a renewable-based multi-energy system. The research presents effective solutions for decreasing carbon emissions and energy expenses, while still remaining profitable. The model offers a cost-efficient and eco-friendly method to accomplish Sustainable Development Goals within the energy industry. Shirmohammadi et al. [29] developed an integrated industrial CO_2 utilization system with renewable source to produce green urea. In addition to environmental benefit of the system, the synthesis of urea improves when ammonia is mixed with captured CO_2, achieving a capacity boost of nearly 8 %. In another study, Sotoodeh et al. [30] developed a polygeneration system in which thermoelectric generators are used to recover the waste heat. This change results in an average power generation increase of 12 %. The proposed system achieved 52.3 % and 41.3 % for energy and exergy efficiencies, respectively. An extensive parametric investigation was also conducted to examine the impact of important design features, finding out that the gasification temperature had the most notable influence on the system's performance.

Moreover, additional studies have evaluated polygeneration systems using exergy and economic evaluation, including CO_2 capture systems [31]. For instance, Shirmohammadi et al. [32] developed a CO_2 liquefaction system for industrial carbon capture and storage (CCS) using waste heat from an ammonia plant stack and analyzed the system from a thermodynamic perspective. The system could liquefy 54.5 tonnes of CO_2 per day, with a coefficient of performance of 0.28 and overall exergy efficiency of 69.7 %. Furthermore, Ismail et al. [33] developed a polygeneration WtE system in which plastic wastes gasification was used to produce syngas via different sub-systems. The system generated power, hydrogen, heating, hot and freshwater, with a reported energy and exergy efficiency of 66.24 % and 48.10 %, respectively.

Building upon these studies, this research focuses on the modeling, analyses, and optimization of a novel polygeneration energy system based on biomass integrated gasification combined cycle (BIGCC). This includes incorporating hydrogen separation, carbon capture and storage (CCS), methanol synthesis, domestic water heating, and multi-stage flash (MSF) desalination. The feasibility of installing the polygeneration plant in Spain is assessed using economic parameters derived from the country's energy system. The study has several key objectives: first, to design an integrated energy system for climate-neutral operation; second, to develop a cutting-edge model for biomass-based distributed energy systems; third, to perform energy-exergy analyses and a technoeconomic evaluation of the proposed system; and fourth, to conduct an optimization based on various cases with the aim of improvement of the system performance. An important aspect of this work is the integration of an MSF unit as a sink for thermal energy that would be otherwise wasted in conventional Rankine cycles. Eventually, a sensitivity analysis is conducted to examine the influence of the main system parameters, ensuring maximum efficiency and flexibility under different operational conditions.

2. System description

The developed system aims to produce various products, utilizing a biomass gasification system as upstream. Fig. 1 shows the schematic of the proposed system. The system features a steam gasifier that converts wood residues into hydrogen-enriched syngas. Additionally, a Brayton WHR system captures heat from the high-temperature syngas to generate electricity. Furthermore, a Rankine cycle is integrated with a MSF desalination unit, functioning as a bottoming cycle to meet electricity and freshwater needs using the residual heat expelled by the Brayton WHR system. The system also includes a separation unit to extract hydrogen from the resulting syngas, a CCS unit for capturing CO_2

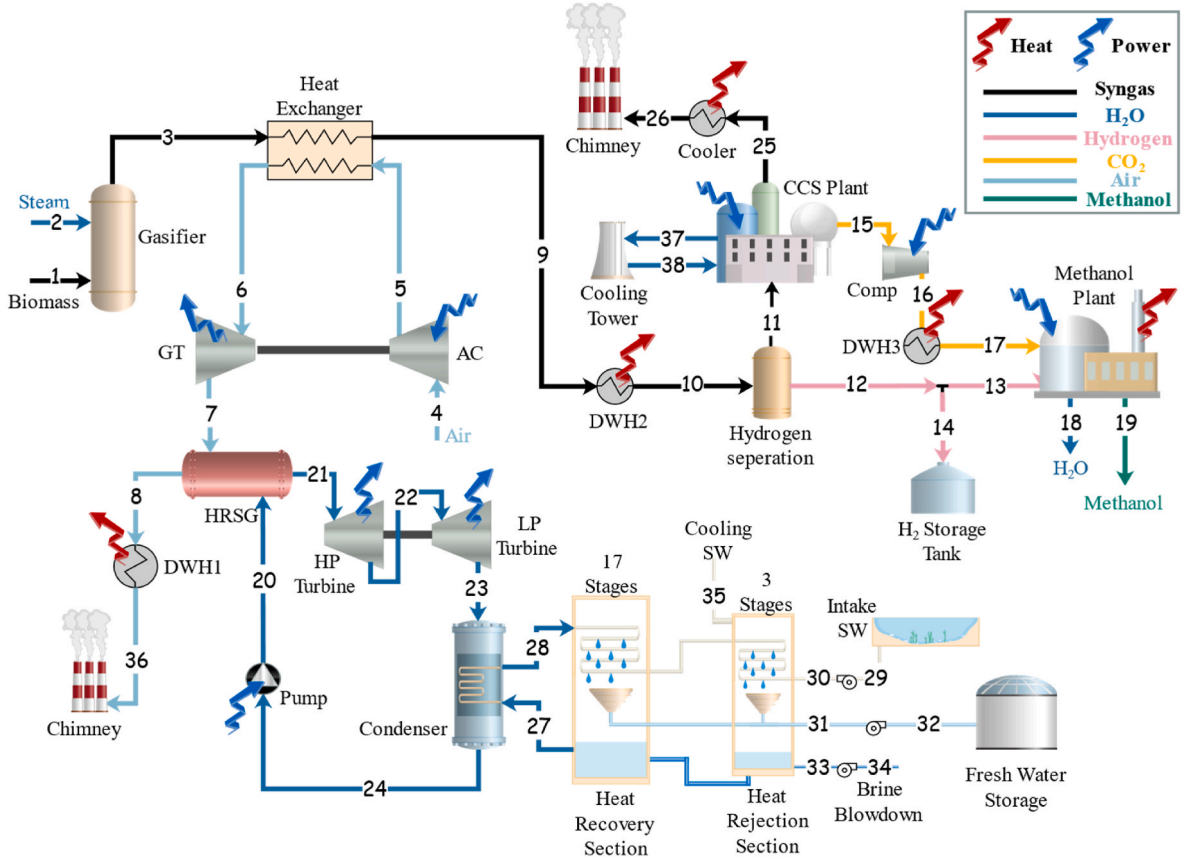

Fig. 1. Schematic of the integrated waste-to-energy system.

from the syngas stream, a methanol synthesis module (MSM), and domestic water heating (DWH) units to recover the excess heat. To conclude, the syngas generated is utilized for producing methanol and hydrogen, both of which are regarded as promising carbon-neutral fuels, in addition to providing power, heat, and freshwater. A detailed description of the developed polygeneration system is described in the following sections.

2.1. Integrated gasification combined cycle

In the developed system, the gasifier generates hydrogen-enriched syngas with high-temperature suitable for H_2 production applications. The generated syngas (line 3) first flows through a heat exchanger, where it transfers heat to the working fluid of the Brayton WHR system (line 5). After passing through the heat exchanger, the syngas is directed to the hydrogen separation unit to produce H_2. In the downstream cycle, the hot air stream (line 6) is fed into a gas turbine (GT) to produce electricity. Next, the exhaust heat from the turbine is sent to the heat recovery steam generator (HRSG), which powers the steam Rankine cycle (line 7), while any residual thermal energy is utilized by the heater for DWH (line 8). In the Rankine cycle, the superheated steam is utilized for producing power through a turbine system (line 21), consisting of a high-pressure (HP) and a low-pressure (LP) part. A condenser removes the stream's remaining heat, which exits the LP turbine (line 23). On the other side, an MSF desalination is implemented as a WHR system bottoming cycle for heat recovery (HR) purposes. The brine water is used to cool the turbine outlet stream and turn it into saturated liquid in the condenser (line 27). Then a pump compresses this saturated liquid again for reaching the high-pressure level (line 24).

2.2. Multi-stage flash desalination

The MSF desalination plant in the proposed system, which includes brine recirculation, is made up of three main parts: the brine heater, which is the condenser of the Rankine cycle, the HR section, and the heat rejection (HJ) section. Both the HR and HJ sections are composed of multiple stages. At each stage, a condenser is present where the vapor is transformed into liquid. The demister is positioned between the flash chamber and the condenser to remove brine droplets from the vapor produced during flashing. Seawater intake ($\dot{m}_f + \dot{m}_{cw}$) circulates within the condenser tubes situated in the HR side, where it absorbs latent heat from condensed freshwater vapor, causing its temperature to rise. Upon reaching the final stage of the initial rejection process, the intake seawater splits into two streams: the cooling seawater ($\dot{m}_{cw}$), which is discharged into the sea, and the feeding seawater ($\dot{m}_f$), which is mixed in the brine pool during the final flashing step in the HR section. The cooling seawater removes excess heat added to the system by the brine heater. In the final stage of the HR section, two streams are collected from the brine pool: blowdown brine and recycle brine. The blowdown brine stream ($\dot{m}_b$) is discharged into the ocean to regulate system salinity. Meanwhile, the recycle brine flow ($\dot{m}_r$) passes through the condenser tubes of the final HR stage, increasing its temperature by absorbing latent heat from condensing freshwater vapor at each stage. Subsequently, the recycled brine stream moves through the brine heater (steam Rankine condenser), where steam turbine outflow ($\dot{m}_s$) condenses on the exterior of the tubes, elevating the recycle brine temperature to the top brine temperature (TBT). During the flashing stages, hot brine flows through multiple stages, producing small amounts of freshwater vapor through brine flashing. The vapor flows through the demister and condenses in the heat exchanger, allowing the cold brine stream to recycle and absorb latent heat from the vaporized freshwater. Finally, the vapor undergoes condensation and accumulates in a distil-

late tray, producing the desired distillate product.

2.3. Hydrogen separation

Due to its high efficiency and minimal energy usage, pressure swing adsorption (PSA) technology is used to deliver the needed H_2 for producing methanol. The PSA operates at room temperature and a pressure range of 1–4 bar. This unit can extract up to 85 % of the hydrogen content from syngas. The unit consists of activated carbon and zeolite membranes, has a cross-section area of 1.6 cm^2, and, based on literature, experiences a pressure drop of approximately 2.5 % [34,35].

2.4. Carbon capture and sequestration

The CCS unit absorbs the syngas in a chemical process. The outcome involves capturing the CO_2. Utilizing the CCS unit results in a notable decline in CO_2 emissions. The CO_2 capture technology employed in this research is based on monoethanolamine (MEA) at a mass concentration of 30 % as the solvent. The CCS specifications are based on Amman [36]. The selected CCS module achieves an 85 % CO_2 capture rate, requiring 44 kWh_{el} of energy for compressing each ton of CO_2. Additionally, the solvent regeneration process requires 3.2 MJ per kilogram of CO_2, and the pressure drop is approximately 5 % in this unit.

2.5. Methanol synthesis module

A portion of the hydrogen extracted from the PSA unit (line 13) and carbon dioxide captured through CCS (line 17) is directed to the methanol synthesis module (MSM). The remaining hydrogen is stored in a storage unit. Thermal energy required for CCS processes is provided by hot water exiting the cooler. The captured CO_2 is condensed and pressurized to blend with hydrogen in the MSM, while high-pressure CO_2 is utilized to extract heat for DWH applications. Based on the design proposed by Kiss et al. [37], the MSM starts by combining the CO_2 stream with recycled high-pressure gas. This mixture flows into the feed effluent heat exchanger (FEHE), where it absorbs heat from the outgoing reactor stream to reach the required temperature before entering the reactor. After passing through the FEHE and an additional cooler, the reactor output enters a separator, where liquid water and methanol are separated from non-condensable gases such as CO, CO_2, and H_2. To maintain optimal reactor pressure, 1.5 % of the recycle stream is diverted to a compressor. The separator directs the liquid to a stripper, which is compressed by a five-stage compressor and combined with the hydrogen intake. One outlet from the stripper is directed to a distillation column, where it is separated into water at the base and methanol at the surface—the main product. The other stream coming from the stripper passes through a condenser, returning liquids to the stripper and sending vapors back to the separator. For a more detailed description on the methanol synthesis process, the readers are referred to Kiss et al. [37].

3. Methodology

3.1. Modeling

The Engineering Equation Solver (EES) software [38] is employed to model the system. In this study, EES built-in libraries and databases, including NASA polynomial functions for thermophysical properties and NIST correlations [39] for modeling gasification processes are employed. For modelling the desalination, we used the seawater library developed at MIT [40,41]. Calculations related to the mass, energy, and exergy balances of the proposed system and its sub-systems are based on a biomass flow of 1 kg/s. Detailed descriptions of reaction kinetics, energy and exergy analysis are provided in the Supplementary Information (Sections S. 1 and S. 2). Moreover, Table 1 summarizes the main inputs of the process.

Table 1
Input data for the design and analysis of the devised polygeneration system [30,34,35,37,42–44].

Subsystem	Parameter	Value	Unit
BIGCC	Gasifier temperature	1473	K
	Steam temperature	673.15	K
	Air compressor inlet temperature	298.15	K
	$TTD_{Heat\ Exchanger}$	5	K
	TTD_{HRSG}	20	K
	TTD_{Heater}	5	K
	Brayton WHR pressure ratio, PR	10	
	Steam Rankine pressure ratio, PRR	200	
MSF	Intake seawater temperature	298.15	K
	Intake seawater salinity	42000	ppm
	Rejected brine salinity	70000	ppm
	MSF total number of stages	20	
	Number of heat rejection stages	3	
MSM	$T_{reactor}$	523	K
	$P_{reactor}$	50	bar
	H_2/CO_2 molar ratio	3	
	Weight of catalyst	865	kg
PSA	Operating temperature	298.15	K
	Operating pressure range	1–4	bar
	Hydrogen recovery efficiency	85	%
	Cross-section area	1.6	cm^2
	Pressure drop	2.5	%
CCS	Capture rate	85	%
	Solvent	MEA solution (30 wt%)	
	Solvent regeneration energy	3.2	MJ/kg_{CO2}
	Energy use for CO_2 compression	44	$kWh/tonne_{CO2}$
	Pressure drop	5	%

3.2. Key performance indicators

The aim of the developed system is to suggest a carbon-neutral, efficient, polygeneration configuration. For this purpose, several indicators arising from the energy and exergy analysis, as well as the environmental evaluation, are selected. From an energetic perspective, the efficiency for the developed system is expressed as:

$$\eta_{en} = \frac{\dot{W}_{Net} + \dot{m}_{14} LHV_{H_2} + \dot{m}_{19} LHV_{CH_3OH} + \dot{Q}_{MSF} + \dot{Q}_{DWH}}{\dot{m}_1 LHV_{biomass} + \dot{Q}_{Steam}} \quad (1)$$

$$\dot{W}_{Net} = \dot{W}_{BWHRS} + \dot{W}_{st} - \dot{W}_{CCS} - \dot{W}_{MSU} - \dot{W}_{CO2Comp} - \dot{W}_{Pumps} \quad (2)$$

$$\dot{Q}_{DWH} = \dot{Q}_{DWH1} + \dot{Q}_{DWH2} + \dot{Q}_{DWH3} + \dot{Q}_{MSU} - \dot{Q}_{Cooler} \quad (3)$$

where LHV_{H_2} and LHV_{CH_3OH} are the lower heating value (LHV) of H_2 and methanol.

Additionally, the exergy efficiency is defined as the ratio of the exergy rate of the product to the fuel:

$$\eta_{ex} = \frac{\dot{W}_{Net} + \dot{E}x_{Product}^{H2} + \dot{E}x_{Product}^{Methanol} + \dot{E}x_{Product}^{Freshwater} + \dot{Q}_{DWH}\left(1 - \frac{T_0}{T_{DWH}}\right)}{\dot{E}x_{Fuel}^{Gasifer}} \quad (4)$$

Where T_{DWH} is DWH temperature, provided to the consumer equal to $T_{DWH} = 373.15\ K$.

Another parameter included is the Sustainability Index (SI), which connects the exergy analysis to the environmental impact [45]. To mitigate the environmental impact, it is crucial to utilize sustainable or renewable sources to have the least depletion of exergy destruction for a proper use of resources. Thus, society can decline its use of resources and extend their lifetimes. In this investigation, SI is used to relate exergy to environmental impact.

$$SI = \frac{1}{DP} \tag{5}$$

where *DP* is the total exergy destruction divided by the exergy of fuel (a depletion number) [46]. The *SI* reveals how reducing exergy destruction in an energy system could result in an environmental impact drop [47].

Finally, the CO_2 Emission Reduction Ratio (CO_2ERR) is considered for environmental assessment of the devised system as frequently used in the literature [48], so as to examine the environmental benefits of polygeneration systems relative to a reference system. The CO_2ERR can be projected, as below:

$$CO_2ERR = 1 - \frac{CO_{2_{tot}}^{Scenario}}{CO_{2_{tot}}^{Benchmark}} \tag{6}$$

where $CO_{2_{tot}}^{Scenario}$ and $CO_{2_{tot}}^{Benchmark}$ are the CO_2 emissions of the considered scenario and benchmark in m^3/h for comparison, respectively.

3.3. Economic analysis

The economic analysis is performed based on the Total Revenue Requirement (TRR) method to evaluate the developed system, considering Spain's energy market serving as the reference for economic parameters. This analysis offers beneficial insights into long-term viability of the system, especially given the integration of multiple energy carriers, including electricity, biomass, and steam. The approach not only takes into account the initial capital investment but also factors in the operational and maintenance costs (OMC) and fuel costs (FC), which reflect the specific conditions of the Spanish energy market. The details of methodology can be found in the literature [49] and only the main equations are retained here. The levelized annual TRR is calculated using the Capital Recovery Factor (CRF):

$$TRR_L = CRF \sum_{1}^{BL} \frac{TRR_j}{(1+i_{eff})^j} \tag{7}$$

where CRF is derived as:

$$CRF = \frac{i_{eff}(1+i_{eff})^{BL}}{(1+i_{eff})^{BL}-1} \quad n = 30 years,\ i = 0.1,\ CRF = 0.1061 \tag{8}$$

TRR_j is obtained with summation of total capital recovery (TCR), return on investment (ROI), FC, and OMC [49]:

$$TRR_j = TCR_j + ROI_j + FC_j + OMC_j \tag{9}$$

In this study, the cost of fuel consists of electricity, wood residues and steam for the developed polygeneration system. The viability of establishing the polygeneration plant in Spain is evaluated using economic parameters derived from the country's energy system, so the market prices of energy carriers in Spain have been considered. The biomass fuel cost includes transportation expenses, as the polygeneration plant is assumed to be located near the biomass source, minimizing logistical costs. Economic inputs and assumptions regarding CRF calculation and market prices are provided in Table 2. All costs are reported in $2024.

Levelized Cost of Electricity (LCOE) gives us information about the average cost of electricity production for the next 30 years and how it is related to the initial investment and the electricity generation [57]. The LCOE of renewable-based energy systems is mainly sensitive to the electricity price and the power load [58]. In order to conduct LCOE for the developed polygeneration system, the generated thermal heat, as well as the produced hydrogen, methanol and desalinated water as by-products of the system, have been considered. The levelized cost of electricity and other products can be individually driven by the following relationship:

$$MPUC_L = \frac{TRR - BPV}{MPQ} \tag{10}$$

where $MPUC_L$ is the levelized main product unit cost, BPV is the by-product value of heat, and MPQ is the main product quantity.

Chemical Engineering Plant Cost Index (CEPCI) is used to update the cost of equipment to different years [59]. The final value of CEPCI is taken as 800.7 (March 2024). The correlations used to calculate the purchase equipment costs are provided in the Supplementary Information (see Section S. 4 and Table S5).

Table 2
Input parameters and assumptions for economic evaluation.

Input parameters	Value	Unit	Reference
Interest rate	10	%	
System lifetime	30	years	
Capital Recovery Factor, CRF	0.1061		
Cost of electricity for Spain	0.1213	$/kWh	[50]
Cost of wood residues	40.6	$/tonne	[51]
Cost of steam	28.3	$/tonne	[52]
Selling price of the heat	0.05	$/kWh	[53]
Selling price of the hydrogen	2.7	$/kg	[54]
Selling price of the methanol	0.39	$/kg	[55]
Selling price of the water	1.96	$/kg	[56]

4. Results and discussion

4.1. Model verification and modeling results

To validate findings in this work, the steam gasifier MSF desalination and MSM results are compared with those found in previous literature. Schuster et al. [60] provided analytical data for validating wood steam gasification in a gasifier at conditions of 1073 K gasification temperature and 25 % moisture content. In the case of MSF, the developed mathematical representation is run based on the specification of that reference paper. Similarly, verification of the MSM model is obtained by comparing the final stream composition with the literature [37]. Table 3 outlines the verification of the gasifier, MSM, and MSF desalination. This comparison reveals strong agreement between the model results of this study and the experimental data from recent literature.

The results of the proposed energy system, comprising the net power, DWH, rate of H_2 and methanol productions, efficiencies, and distilled water rate can be found in Table 4. The energy and exergy efficiencies of the developed polygeneration system are found to be 55.22 % and 37.92 %, respectively, which is higher than the conventional power generation systems. As Table 4 shows, the Brayton WHR system is 1021 kW. The electricity consumed by the chemical facilities is about 630.3 kW, which is less than half of the total produced power. The amount of thermal energy produced by the developed system is 1730 kW. Eventually, the hydrogen and methanol production rates are 0.02838 kg/s and 0.15 kg/s.

4.2. Exergy analysis

A detailed breakdown of operational conditions and exergy flows for each stream in the developed system is provided in Table S4 of the Supplementary Information. Fig. 2 shows the extent to which each equipment contributes to the overall exergy destruction rate.

In terms of exergy analysis, the gasifier and HRSG are responsible for the highest amount of exergy destruction in the total system, with 2.552 MW and 2.305 MW, respectively. For the gasifier, this is due to irreversible chemical reactions, significant temperature gradients, entropy generation, and incomplete conversion of the feedstock. For the HRSG, within the Rankine Cycle, the main reasons for the exergy destruction are the large temperature gradients involved in heat recovery, inefficiencies in the multi-stage heat exchange process, pressure and temperature losses and the inherent irreversibility of heat transfer from lower-quality heat sources. MSM, with the amount of 1.4 MW, generates

Table 3
Model validation results.

Subsystem	Data comparison						
Steam Gasifier	**Component**	**Hydrogen**	**Carbon monoxide**	**Carbon dioxide**	**Water**	**Methane**	**Nitrogen**
	Present study	46.81 %	24.54 %	10.27 %	18.3 %	0.082 %	0 %
	Schuster et al. [60]	46.57 %	25.84 %	10.30 %	17.11 %	0.09 %	0 %
MSF Desalination			**Parameter**				***TPR***
			Present study				6.7
			El-Dessouky et al. [43]				6.68
MSM	**Component**	**Hydrogen**	**Carbon monoxide**	**Carbon dioxide**	**Water**		**Methanol**
	Present study	63.74 %	3.379 %	22.62 %	4.921 %		5.337 %
	Kiss et al. [37]	63.95 %	3.24 %	22.78 %	4.74 %		5.2 %

Table 4
Final results of the proposed system.

Key outcomes of the devised system	Value	Unit
$\dot{W}_{Brayton\ WHR}$	1021	kW
$\dot{W}_{st}$	552.7	kW
$\dot{Q}_{DWH}$	1730	kW
$\dot{m}_{H2}$	0.02838	Kg/s
$\dot{m}_{CO2}$	0.2419	Kg/s
$\dot{m}_{Methanol}$	0.15	Kg/s
$\dot{m}_{Distilled\ water}$	3.644	Kg/s
$\dot{W}_{Net}$	943.4	kW
CO_2 emission	76.61	m^3/h
SI	3.219	
η_{en}	55.22	%
η_{ex}	37.92	%

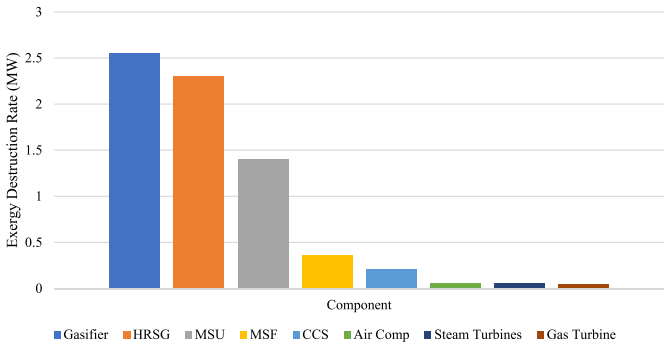

Fig. 2. Share of each equipment in terms of exergy destruction in the developed system.

a considerable amount of exergy destruction among the components of the system. In contrast, pumps, heat exchangers, and PSA make the smallest impact on overall exergy destruction.

4.3. Economic results

Using the TRR method, the TRR_L, which represents the total annualized cost required by the system, is calculated to be $4.7 million. This value ensures that the initial capital investment and operational expenses are fully recovered throughout the lifespan of the project. Table S8 provided the amount of TRR, OPC, and FC for the benchmark system in thousand $ (2024).

Fig. S2 shows the levelized cost of each product generated by the polygeneration system. The results for the LCOE, LCOH, $LCOH_2$, LCOM and LCOW are 0.08 $/kWh, 0.04 $/kWh, 2.43 $/kg, 0.33 $/kg, and 0.12 $/$m^3$, respectively. These results are compared with similar technologies in the literature in Table 5. The LCOE cost 0.08 $/kWh is viable in the market of Spain compared to the present electricity cost of 0.1213

Table 5
Comparison of the levelized cost of products with those of other studies.

Product	Reference	Technology/System Description	Levelized Cost	Unit
Methanol	Soltanieh et al. [62]	Coproduction of electricity and methanol through renewable hydrogen and CO_2 capture	0.576	$/kg
	Chen et al. [63]	Renewable methanol production	1.459	
	Hi et al. [64]	Trigeneration system using LFG	0.124	
	Present study	WtE polygeneration system	0.33	
Hydrogen	Farhat and Reichelstein [65]	Hydrogen-based polygeneration	1.373	$/kg
	Tera et al. [66]	Polygeneration system based on biomass gasification, SOFC and waste heat recovery.	4.06	
	Wang et al. [67]	Solar-wind driven ethanol steam reforming via a membrane reactor with biomass feedstock	4.16	
	Present study	WtE polygeneration system	2.43	
Electricity	Ghema et al. [68]	WHR-based polygeneration system	0.17	$/kWh
	Ray and De [69]	Solar, biomass and wind resources are the inputs to the considered polygeneration system	0.1081	
	Present study	WtE polygeneration system	0.08	
Heating	Ghema et al. [68]	WHR-based polygeneration system	0.13	$/kWh
	Shirmohammadi et al. [50]	Solar-assisted CO_2 capture system	0.0359	
	Present study	WtE polygeneration system	0.04	
Freshwater	Shabaan [70]	Integrated Solar Combined Cycle with a Multi Stage Flash (MSF) desalination unit	0.54	$/$m^3$
	Present study	WtE polygeneration system	0.12	

$/kWh, highlighting the system's potential thanks to its affordable electricity, which is crucial considering Spain's dedication to decarbonizing its energy sector [61]. Likewise, the LCOH cost 0.04 $/kWh closely aligns with the one reported in Table 5, which examines various regions with high solar energy potential, specifically in the context of a parabolic trough-assisted carbon capture system [50]. Consequently, the polygeneration plant is able to deliver thermal energy at a promising price point compared to other sources. This level of heat generation could be beneficial for businesses and local governments looking for effective district heating options, which are becoming more important as Europe shifts towards more sustainable energy systems.

Moreover, the results related to BPV emphasize the economic viability of the developed system. The $LCOH_2$, with an amount of 2.43 $/kg, presents an acceptable value given Spain's extensive investment in this sector, being in the range of competitive standards of hydrogen production. Since the need for hydrogen as a clean fuel has been increased in transportation and industry, such a system can support Spain's aim at green hydrogen production [71]. The LCOM, with an amount of 0.33 $/kg, also proves its great potential, as it helps to diminish the dependency of Spain on imports of this fuel and provides robust energy security, endorsing local production of such fuels. This value also aligns well with the cost of methanol produced by the trigeneration system utilizing LFG, as reported in Table 5. Finally, LCOW presents a cost of 0.12 $/$m^3$, highlighting the capacity of the system to provide desalinated water at a reasonable price. This significant cost reduction is largely attributed to the utilization of waste heat, which minimizes the energy demand for desalination and lowers the overall water production cost. Additionally, when more waste heat becomes available in the condenser, it enhances the desalination process, increasing freshwater production at lower cost. Considering the water scarcity problems in the Spanish Mediterranean area and south Spain, especially in areas like Malaga, this feature greatly enhances the system's appeal, especially for coastal regions dealing with a lack of freshwater.

4.4. Parametric analysis

This section analyzes the impact of the main design parameters listed in Table 1. These parameters include the gasifier temperature and the pressure ratios of the Brayton and Rankine cycles. The analysis focuses on their influence on the production rates of energy carriers (hydrogen and methanol), freshwater output, and overall energy and exergy efficiency. Parametric study is done by changing each key parameter while keeping the rest constant, so as to isolate the effect of each variable.

4.4.1. Impact of gasification temperature

The impact of the temperature of gasification is studied by changing its value from 1173 to 1473 K. Fig. 3a shows the impact of the gasifier temperature on the methanol and hydrogen production rates along with distilled water production. Based on this figure, as the gasifier temperature increases, hydrogen and methanol production rates increase as well as freshwater, but at a higher pace. In syngas composition, as gasification temperature goes up, water content increases, while the content of hydrogen decreases. Although the hydrogen content in the syngas decreases at higher temperatures, the overall stored hydrogen increases due to reduced methanol production in the MSM unit. Therefore, both methanol and hydrogen production ultimately rise with temperature, but at varying rates. Additionally, freshwater production increases continuously with temperature.

Fig. 3b shows the trends in net generated power and domestic water heating as the gasifier temperature changes. As illustrated, both net generated power and domestic water heating increase with higher gasifier temperatures. The increase in net power generation occurs because higher gasifier temperatures raise the available heat in the system, thus increasing the energy supplied to the Brayton and Rankine cycles. Similarly, the increase in DWH is attributed to the additional heat

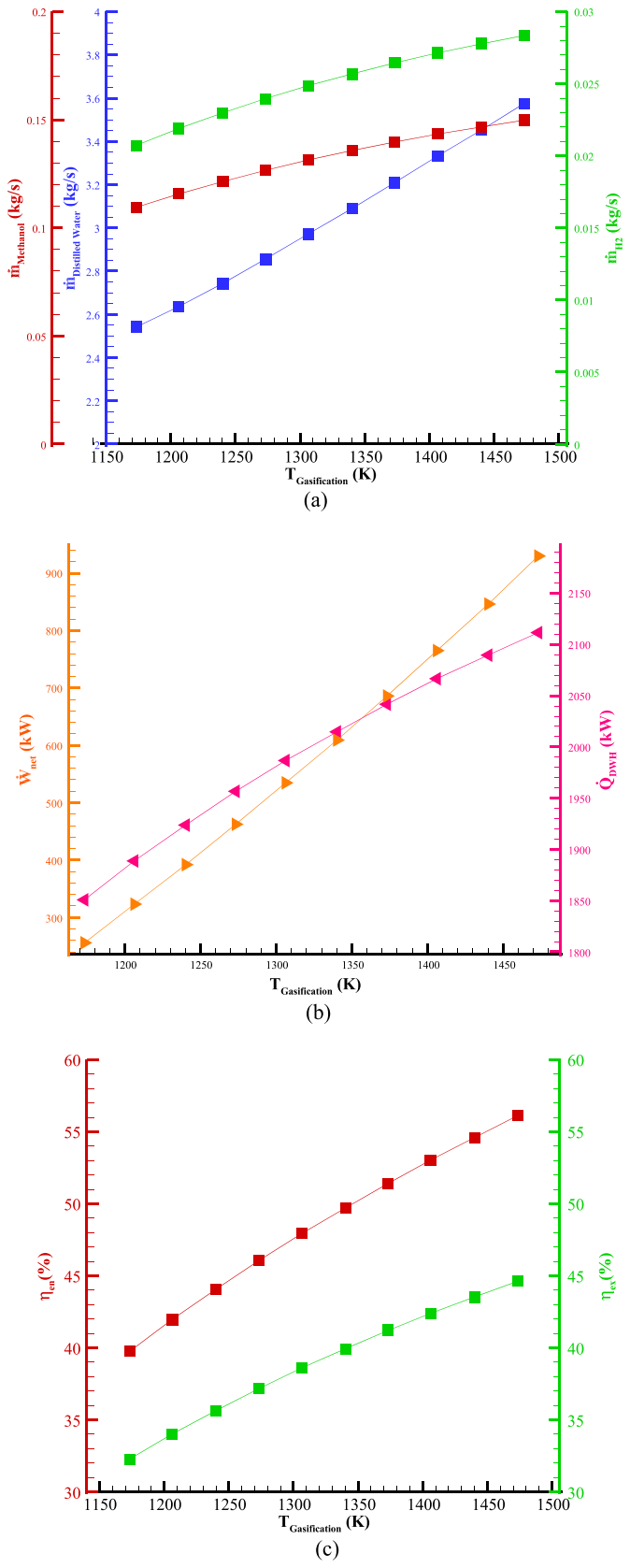

Fig. 3. Influence of gasifier temperature on: (a) distilled water ($\dot{m}_{Distilled\ Water}$), hydrogen ($\dot{m}_{H2}$), and methanol ($\dot{m}_{Methanol}$) production rates, (b) net power ($\dot{W}_{net}$) and domestic water heating ($\dot{Q}_{DWH}$) production rates, (c) energy (η_{en}) and exergy (η_{ex}) efficiencies.

generated by both the MSM and DWH units.

Fig. 3c presents the effect of the gasifier temperature on the energy and exergy key performance indicators of the Polygeneration system. Both energy and exergy efficiencies increase with the gasifier temperature up to 57 and 45 % respectively at 1473 K. However, the slower growing rate of the exergy efficiency indicates that the increase in input energy is not completely converted into useful exergy output.

4.4.2. Impact of Brayton WHR pressure ratio

In this part, the Brayton pressure ratio (PR) influence on the system is investigated in an interval of 5–15. Fig. 4a shows how PR impacts the production rates of methanol, hydrogen, and distilled water. Based on this figure, hydrogen and methanol production rates remain constant, as they depend solely on the syngas temperature leaving the heat exchanger (HX), which does not change with PR. In contrast, freshwater production decreases as PR increases. This decline occurs because a higher PR leads to lower gas turbine outlet temperatures, reducing the available excess heat.

The effect of PR on the net generated power and domestic water heating is shown in Fig. 4b. An increase in PR negatively affects power generation due to the higher power demand of the compressor. Additionally, higher pressure drops in the turbine lead to a lower outlet temperature, which is the primary reason for the decline in Rankine cycle power generation. Moreover, a higher enthalpy of the air entering the heater due to lower pressure further reduces the efficiency of Rankine cycle. However, since DWH significantly increases, the overall exergy efficiency continues to rise up to 37.8 % at a PR of 15 bar, while the energy efficiency remains constant, as shown in Fig. 4c.

4.4.3. Impact of Rankine pressure ratio

The influence of the steam Rankine cycle pressure ratio (PRR) is evaluated in Fig. 5. As observed in the previous subsection with the Brayton cycle, hydrogen and methanol production rates remain unchanged when PRR increases, while more waste heat becomes available in the condenser. This additional thermal energy is utilized by the desalination system, leading to increased freshwater production (see Fig. 5a).

According to Fig. 5b, higher PRR results in significant increase in the net power output, particularly enhancing the production of HP turbine, which follows a parabolic trend (orange line). This behavior is due to the exponential rise in the MSM power demand. On the other hand, the heat output experiences only a slight increase. Fig. 5c shows that efficiencies are only modestly affected by the PRR, indicating that the PRR has a low impact on the overall system performance.

4.5. Optimization study

A proper mathematical code is developed in the engineering equation solver software to simulate and optimize the examined system. For this purpose, a genetic algorithm has been employed [72], whose parameter details are listed in Table 6.

The optimization procedure is carried out by selecting all independent parameters that could impact the outcomes of the process. They include the gasifier temperature and pressure ($T_{Gasification}$, $P_{Gasification}$), the temperature of the injected steam to the gasifier (T_2), the Brayton pressure ratio (PR), the inlet air temperature in Brayton WHR system (T_4), the Rankine pressure ratio (PRR), the Rankine condenser pressure (P_{Cond}), and the thermal temperature difference of HRSG (TTD_{HRSG}) and heat exchanger (TTD_{HX}). Next, the proper boundary for each of these variables and guess values are defined. The main goal is to optimize a single parameter in each mode as an objective function [73].

In this study, multiple objective functions have been considered for the developed system with the individual boundary conditions. The objective functions by which the system examined are maximization of net power, energy and exergy efficiencies as well as sustainability and CO_2 emission minimization. Based on these different functions, the key

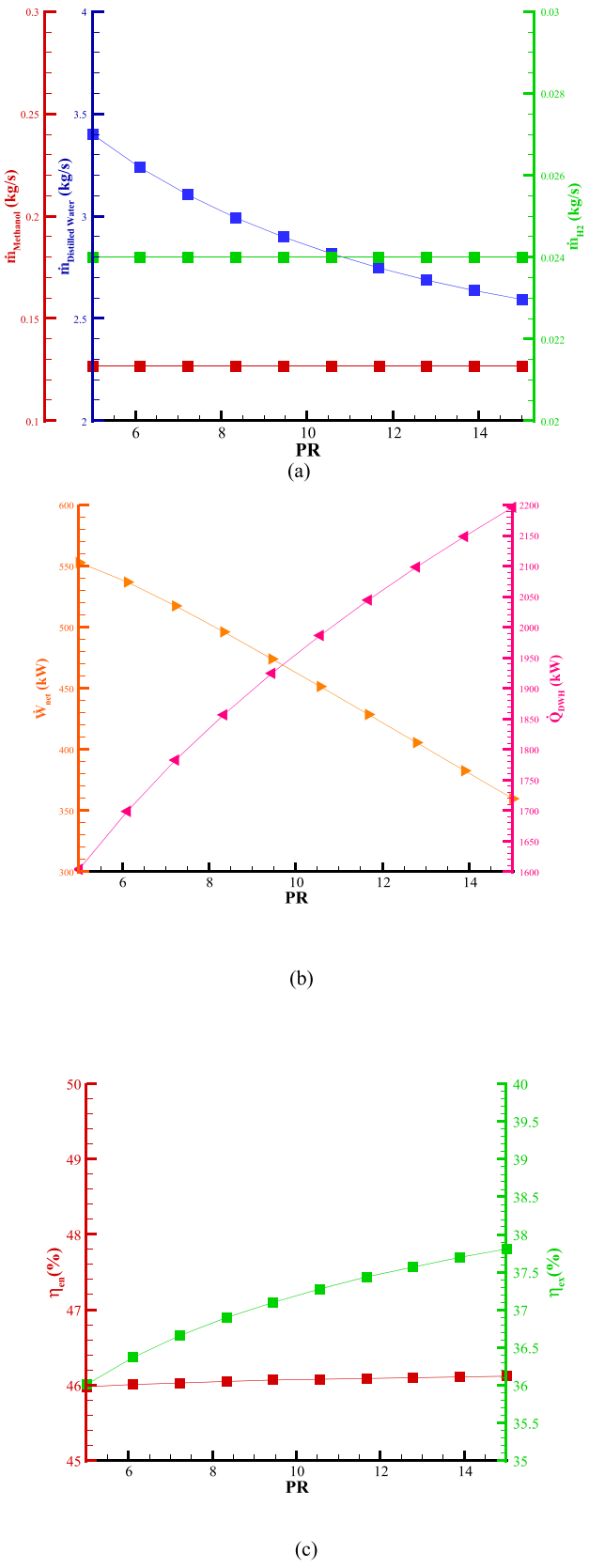

Fig. 4. Influence of the Brayton WHR pressure ratio (PR) on: (a) distilled water ($\dot{m}_{Distilled\ Water}$), hydrogen ($\dot{m}_{H2}$), and methanol ($\dot{m}_{Methanol}$) production rates, (b) net power ($\dot{W}_{net}$) and domestic water heating ($\dot{Q}_{DWH}$) production rates, (c) energy (η_{en}) and exergy (η_{ex}) efficiencies.

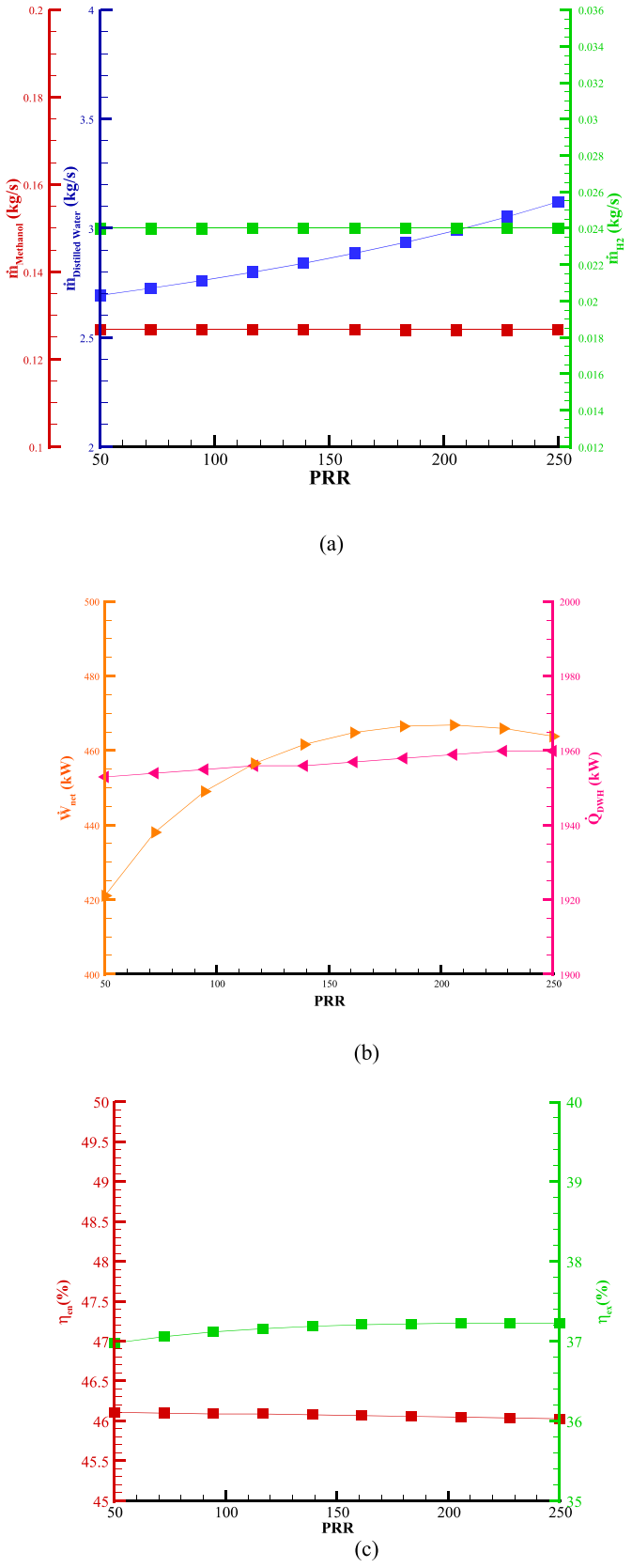

Fig. 5. Impact of the steam Rankine pressure ratio (PRR) on: (a) distilled water ($\dot{m}_{Distilled\ Water}$), hydrogen ($\dot{m}_{H2}$), and methanol ($\dot{m}_{Methanol}$) production rates, (b) net power ($\dot{W}_{net}$) and domestic water heating ($\dot{Q}_{DWH}$) production rates, (c) energy (η_{en}) and exergy (η_{ex}) efficiencies.

Table 6
Assumptions and configuration parameters used in the genetic algorithm optimization [73–75].

Parameter	Value
Population size	32
Number of generations	64
Mutation rate range	0.0005–0.2625
Initial mutation rate	0.25
Crossover probability	0.85

outcomes of the devised system are presented in Table 7.

When the amount of power produced by the devised system is taken as the function to minimize, a maximum net power of 1092 output kW could be attained. This comes at the cost of maximizing the gasifier temperature (1473 K) and the Rankine Pressure Ratio (247.9), resulting in higher CO_2 emissions (see Table 7). Details on the boundary ranges and corresponding optimal values of all parameters studied, are given in Table S9.

Similarly, in order to investigate the efficiency improvements, the same variables and ranges were considered. The maximum energy efficiency of 67.58 % is attained at the highest gasifier temperature (1473 K), a relatively high Brayton pressure ratio (12.8), and a low Rankine pressure ratio (65.17), as shown in Table S10 ("Opt. η_{en} case "). In this scenario, net power production (798.2 kW) and distilled water output (3.305 kg/s) are significantly reduced, representing a trade-off between maximizing energy efficiency and the production of other useful outputs. However, it must be noted that higher production rates for hydrogen (0.03612 kg/s) and methanol (0.1909 kg/s) are achieved based on the energy efficiency condition.

To explore the maximum exergy efficiency of the devised system, another optimization is executed. The optimal exergy efficiency of 47.11 % was again achieved at maximum gasifier temperature (1473 K), with intermediate Brayton pressure ratio (8.149) and significantly high Rankine pressure ratio (243.6) (see Table S10, "Opt. η_{ex} case"). Achieving this scenario moderately reduces net power output (1018 kW) compared to the power maximization scenario, but results in lower CO_2 emissions (55.87 m^3/h) and moderate distilled water production (3.875 kg/s) (see Table 7). Thus, this case offers a balance between resource efficiency and system productivity.

To achieve the highest sustainability, the same optimization variables were used. The highest sustainability index of 4.802, indicating the lowest exergy destruction with respect to the exergy of fuel, is reached by setting moderate gasifier temperature (1254 K), the highest Brayton pressure ratio (15), and lower Rankine pressure ratio (60.14), as shown in Table S11. Despite the significantly improved sustainability performance, in this scenario the net power output (291.9 kW) and freshwater production (2.324 kg/s) are drastically reduced. Thus, the improvement in sustainability involves considerable trade-offs regarding production outputs, clearly highlighting the difficulty in simultaneously achieving high sustainability and productivity.

As the devised system utilizes wood residues as feedstock, the CO_2 emissions are inherently low, especially since most of the CO_2 generated is captured and utilized for methanol synthesis. Nevertheless, a small fraction of CO_2 is still released into the atmosphere. As a final case, an assessment based on minimizing the CO_2 emissions is carried out by determining the CO_2ERR. The results reveal reaching the lowest CO_2 emissions (55.18 m^3/h) required setting the gasifier at its lowest temperature (1173 K), moderate Brayton pressure ratio (7.024), and lower Rankine cycle pressure ratio (76.05) as indicated in Table S12. Although in this scenario the lowest environmental impact can be obtained, it significantly compromises net power output (275.2 kW) and moderately reduces distilled water production (2.604 kg/s).

Overall, these optimization results clearly illustrate important trade-offs that arise when prioritizing specific operational objectives. They highlight the complexity of simultaneously achieving maximum

Table 7
Key outcomes of the devised system for different objective functions.

Optimized value	Objective				
	Net power maximization	Energy efficiency maximization	Exergy efficiency maximization	Sustainability maximization	CO_2 emission minimization
$\dot{Q}_{DWH}$, kW	1613	2422	1999	2268	1798
$\dot{m}_{H2}$, kg/ s	0.03087	0.03612	0.03596	0.03619	0.03615
$\dot{m}_{Methanol}$, kg/ s	0.1613	0.1909	0.1901	0.1913	0.1911
$\dot{m}_{Distilled\ water}$, kg/ s	4.283	3.305	3.875	2.324	2.604
$\dot{W}_{Net}$, kW	1092	798.2	1018	291.9	275.2
CO_2 emission, m^3/h	69.81	55.88	55.87	55.24	55.18
SI	3.074	4.682	4.262	4.802	4.394
η_{en}, %	59.94	67.58	66.77	61.67	60.08
η_{ex}, %	41.35	46.64	47.11	44.19	43.72

productivity, high efficiency, enhanced sustainability, and minimized environmental impact. Among all cases, the maximization of the exergy efficiency appears to better balance between production, new power and CO_2 emissions.

5. Concluding remarks

In this work, a polygeneration system was developed to utilize waste biomass and generate power, fuel, heating and freshwater. The system integrates a steam gasifier, a biomass integrated gasification combined cycle (BIGCC), a methanol synthesis unit (MSM), a multi-stage flash (MSF) desalination unit, and a domestic water heating (DWH) application. A comprehensive thermodynamic, exergy, and economic analysis was performed to evaluate the system's performance and identify areas for optimization. The significance of the critical operational parameters was thoroughly analyzed through an in-depth investigation of system variables. Eventually, an optimization study was conducted, employing various strategies to enhance system performance.

The results for the base case indicate that the proposed system can produce 943.4 kW of net power, 1730 kW of thermal energy for domestic heating, 3.64 kg/s of freshwater, 0.028 kg/s of hydrogen and finally 0.15 kg/s of methanol. Despite achieving a notable energy efficiency of 55.22 % and overall exergy efficiency of 37.92 % for the proposed system, it depicts significant exergy destruction, with a total rate of 7114.7 kW. The majority of this destruction occurs in the gasifier and HRSG, indicating key areas for further modification and optimization. The economic analysis shows that the levelized costs are competitive, with electricity (LCOE) at 0.08 $/kWh and heat (LCOH) at 0.04 $/kWh. The levelized costs for hydrogen ($LCOH_2$), methanol (LCOM), and water (LCOW) are 2.43 $/kg, 0.33 $/kg, and 0.12 $/$m^3$, respectively. These results suggest that the system could be economically viable, although further cost reductions and optimization may enhance its attractiveness.

From the parametric study, it was found that increasing the gasification temperature was found to enhance hydrogen and distilled water production rates, net power output, and both energy and exergy efficiencies. This improvement is attributed to the increased syngas lower heating value (LHV) and better thermodynamic performance at higher temperatures. Adjusting the Brayton WHR pressure ratio showed that higher pressure ratios reduce net power output and freshwater production due to increased compressor work and lower turbine outlet temperatures, but they enhance exergy efficiency and domestic heating. Increasing the Rankine pressure ratio leads to higher distilled water production and net power output, with a modest positive effect on system efficiencies.

Finally, the system was further optimized based on different criteria from the selected Key Performance Indicators using a genetic algorithm. Optimization for net power maximization led to a maximum output of 1092 kW. Separate optimization for energy and exergy efficiency resulted in improvements to 67.58 % and 47.11 %, respectively, while the highest sustainability index achieved was 4.802, and CO_2 emissions were minimized to 55.18 m^3/h. These results demonstrate that optimizing key operational parameters can significantly enhance system performance, although maximization of the exergetic efficiency provides the most balanced results in terms of production, net power output and CO_2 emissions. The feasibility of the system is reinforced by these optimized outcomes, which indicate improved efficiencies and attractive production rates of energy carriers and products. However, the economic attractiveness of the system depends on the competitiveness of the production costs and the market demand. The levelized costs obtained are within reasonable ranges but may require further optimization and cost reduction to ensure market competitiveness.

In conclusion, the developed system offers a promising approach for the efficient and sustainable conversion of waste biomass into multiple valuable products. The system's performance can be significantly enhanced through optimization of operational parameters, particularly by reducing exergy destruction in the gasifier and HRSG. Further research is intended to explore regional economic assessments and life cycle analysis in detail, investigate dynamic performance optimization strategies, and evaluate the potential for integration with other renewable energy technologies. The system's ability to simultaneously produce various energy carriers makes it a versatile solution that enhances energy diversification and supports sustainability goals. It has the potential for expansion to other regions with abundant biomass, similar WtE potentials, and a need for potable water and fuels.

CRediT authorship contribution statement

Farzin Ahmadi: Writing – review & editing, Writing – original draft, Visualization, Validation, Software, Methodology, Investigation, Formal analysis, Data curation, Conceptualization. **Reza Shirmohammadi:** Writing – review & editing, Writing – original draft, Visualization, Methodology, Investigation, Formal analysis. **Fèlix Llovell:** Writing – review & editing, Resources, Methodology. **Majid Amidpour:** Supervision, Resources, Project administration.

Declaration of competing interest

The authors declare that they have no known competing financial interests or personal relationships that could have appeared to influence the work reported in this paper.

Acknowledgment

Reza Shirmohammadi acknowledges the Juan de la Cierva Fellowship Grant No. JDC2023-050548-I from the Agencia Estatal de Investigación (AEI), funded by MCIU/AEI/10.13039/501100011033 and by the FSE+.

Nomenclature

Symbol

CO_2ERR	CO_2 emission reduction ratio
C_p	Constant-pressure specific heat, kJ kg^{-1} K^{-1}
DP	Depletion number
E_a	Activation energy, J mol^{-1} K^{-1}
$\dot{E}x$	Exergy rate, kW
G	Gibbs energy, kJ $kmol^{-1}$
h	Specific enthalpy, kJ kg^{-1}
K	Equilibrium constant
LHV	Low heating value, kJ kg^{-1}
$\dot{m}$	Mass flow rate, kg s^{-1}
m	Steam molar ratio
M	Molecular weight
MC	Moisture content
n	Mole amount
P	Pressure, bar
PR	Pressure ratio
$\dot{Q}$	Heat rate, kW
R	Universal gas constant, 8.314 kJ/kmole K
SI	Sustainability Index
$STBM$	Mass-based team-to-biomass ratio
T	Temperature, K
T_0	Environment temperature, K
TPR	Thermal performance ratio
T_{st}	Flashing brine temperature drop per stage
TTD	Thermal temperature difference
U	Heat transfer coefficient
W	Power, kW
w	Moisture content
X	Salinity, ppm

Greek letters

η	Efficiency (%)
λ	Latent heat
ϕ	Energy availability of the heat stream (kW)

Superscript and superscript

b	Blowdown brine
$Comp$	Compressor
$Cond$	Condenser
cw	Cooling seawater
D	Destruction
en	Energy
eq	Equilibrium
$Evap$	Evaporator
ex	Exergy
F	Fuel
f	Feed seawater
g	Gasifier
Gen	Generator
H	Hot
HX	Heat exchanger
i	ith component
in	Input stream
is	Isentropic
j	Number of rejection stages
L	Levelized
M	Mean
n	Number of total stages
out	Output stream
p	Product
r	Recycle brine

ref	Reference
s	Motive steam
st	Steam Rankine cycle
tot	Total
Tur	Turbine
vap	Vaporization

Abbreviations

AC	Air compressor
BIGCC	Biomass integrated gasification combined cycle
BPV	By-product value
CEPCI	Chemical engineering plant cost index
CCS	Carbon capture and storage
CRF	Capital recovery factor
DWH	Domestic water heating
EES	Engineering Equation Solver
FEHE	Feed effluent heat exchanger
FC	Fuel cost
GT	Gas turbine
HHV	Higher heating value
HJ	Heat rejection section
HP	High pressure
HRSG	Heat recovery steam generators
LCOE	Levelized cost of electricity
LCOH	Levelized cost of heat
$LCOH_2$	Levelized cost of hydrogen
LCOM	Levelized cost of methanol
LCOW	Levelized cost of water
LP	Low pressure
MSF	Multi-stage flash desalination
MSM	Methanol synthesis module
OMC	Operational and maintenance cost
PR	Brayton pressure ratio
PRR	Steam Rankine cycle pressure ratio
PSA	Pressure swing adsorption
ROI	Return on investment
RWGS	Reverse water gas shift
TBT	Top brine temperature
TRR	Total revenue requirement
WHR	Waste heat recovery
WtE	waste-to-energy

Appendix A. Supplementary data

Supplementary data to this article can be found online at https://doi.org/10.1016/j.renene.2025.123597.

References

[1] D. Shindell, C.J. Smith, Climate and air-quality benefits of a realistic phase-out of fossil fuels, Nature 573 (7774) (2019) 408–411, https://doi.org/10.1038/s41586-019-1554-z.

[2] A.K. Rathoure, S.M. Khade, *Biomass and Bioenergy Solutions for Climate Change Mitigation and Sustainability* (Biomass and Bioenergy Solutions for Climate Change Mitigation and Sustainability), 2022, pp. 1–412.

[3] S. Pavlovic, R. Loni, E. Bellos, D. Vasiljević, G. Najafi, A. Kasaeian, Comparative study of spiral and conical cavity receivers for a solar dish collector, Energy Convers. Manag. (2018), https://doi.org/10.1016/j.enconman.2018.10.030. Article.

[4] I.E. Agency, World Energy Outlook 2018, International Energy Agency Paris, 2018.

[5] M.L.N.M. Carneiro, M.S.P. Gomes, Energy, exergy, environmental and economic analysis of hybrid waste-to-energy plants, Energy Convers. Manag. 179 (2019) 397–417, https://doi.org/10.1016/j.enconman.2018.10.007, 2019/01/01/.

[6] R. Medina-Mijangos, S. Contelles-Rodríguez, H. Guerrero-García-Rojas, L. Seguí-Amórtegui, Waste to energy plant in Spain: a case study using technoeconomic analysis, in: A.E.-F. Abomohra, Q. Wang, J. Huang (Eds.), Waste-to-Energy: Recent Developments and Future Perspectives towards Circular Economy, Springer International Publishing, Cham, 2022, pp. 539–576.

[7] P. Wienchol, A. Szlęk, M. Ditaranto, Waste-to-energy technology integrated with carbon capture – challenges and opportunities, Energy (Calg.) 198 (2020) 117352, https://doi.org/10.1016/j.energy.2020.117352, 2020/05/01/.

[8] A.T. Hoang, et al., Perspective review on municipal solid waste-to-energy route: characteristics, management strategy, and role in circular economy, J. Clean. Prod. 359 (2022) 131897.

[9] A.H. Khan, et al., Current solid waste management strategies and energy recovery in developing countries - state of art review, Chemosphere 291 (2022) 133088, https://doi.org/10.1016/j.chemosphere.2021.133088, 2022/03/01/.

[10] H.D. Beyene, A.A. Werkneh, T.G. Ambaye, Current updates on waste to energy (WtE) technologies: a review, Renew. Energy Focus 24 (2018) 1–11, https://doi.org/10.1016/j.ref.2017.11.001, 2018/03/01/.

[11] A. Kumar, D. Jones, M. Hanna, Thermochemical biomass gasification: a review of the current status of the technology, Energies 2 (3) (2009) 556–581.

[12] Z. Ghaffarpour, M. Mahmoudi, A. Mosaffa, L.G. Farshi, Thermoeconomic assessment of a novel integrated biomass based power generation system including gas turbine cycle, solid oxide fuel cell and rankine cycle, Energy Convers. Manag. 161 (2018) 1–12.

[13] T. Schulzke, Biomass gasification: conversion of forest residues into heat, electricity and base chemicals, Chem. Pap. 73 (8) (2019) 1833–1852, https://doi.org/10.1007/s11696-019-00801-1, 2019/08/01.

[14] H. Amiri, A.F. Sotoodeh, M. Amidpour, A new combined heating and power system driven by biomass for total-site utility applications, Renew. Energy 163 (2021/01/01/2021) 1138–1152, https://doi.org/10.1016/j.renene.2020.09.039.

[15] S. Kaza, L. Yao, P. Bhada-Tata, F. Van Woerden, What a Waste 2.0: a Global Snapshot of Solid Waste Management to 2050, World Bank Publications, 2018.

[16] S. Alzate, B. Restrepo-Cuestas, and Á. Jaramillo-Duque, "Municipal solid waste as a source of electric power generation in Colombia: a techno-economic evaluation under different scenarios," Resources, vol. 8, no. 1, doi: 10.3390/resources8010051.

[17] I.-R. Istrate, E. Medina-Martos, J.-L. Galvez-Martos, J. Dufour, Assessment of the energy recovery potential of municipal solid waste under future scenarios, Appl. Energy 293 (2021) 116915, https://doi.org/10.1016/j.apenergy.2021.116915, 2021/07/01/.

[18] M. Calero, V. Godoy, C.G. Heras, E. Lozano, S. Arjandas, M. Martín-Lara, Current state of biogas and biomethane production and its implications for Spain, Sustain. Energy Fuels 7 (15) (2023) 3584–3602.

[19] S. Farzad, M.A. Mandegari, M. Guo, K.F. Haigh, N. Shah, J.F. Görgens, Multi-product biorefineries from lignocelluloses: a pathway to revitalisation of the sugar industry? Biotechnol. Biofuels 10 (1) (2017) 87, https://doi.org/10.1186/s13068-017-0761-9, 2017/04/11.

[20] Fundación Naturgy "Biogas and biomethane as a key lever in the decarbonization of the Spanish economy." Fundación Naturgy. https://www.fundacionnaturgy.org/en/producto/biogas-andbiomethane-as-a-key-lever-in-the-decarbonization-of-thespanish-economy (accessed.

[21] J. Hernández-Santoyo, A. Sánchez-Cifuentes, Trigeneration: an alternative for energy savings, Appl. Energy 76 (1–3) (2003) 219–227.

[22] G. Chicco, P. Mancarella, Distributed multi-generation: a comprehensive view, Renew. Sustain. Energy Rev. 13 (3) (2009) 535–551.

[23] A. Rong, R. Lahdelma, Role of polygeneration in sustainable energy system development challenges and opportunities from optimization viewpoints, Renew. Sustain. Energy Rev. 53 (2016) 363–372, https://doi.org/10.1016/j.rser.2015.08.060, 2016/01/01/.

[24] M. Ostadi, L. Bromberg, D.R. Cohn, E. Gençer, Flexible methanol production process using biomass/municipal solid waste and hydrogen produced by electrolysis and natural gas pyrolysis, Fuel 334 (2023) 126697, https://doi.org/10.1016/j.fuel.2022.126697, 2023/02/15/.

[25] C. Hakandai, H. Sidik Pramono, M. Aziz, Conversion of municipal solid waste to hydrogen and its storage to methanol, Sustain. Energy Technol. Assessments 51 (2022) 101968, https://doi.org/10.1016/j.seta.2022.101968, 2022/06/01/.

[26] Y. Amirhaeri, F. Pourfayaz, H. Hadavi, A. Kasaeian, Energy and exergy analysis-based monthly co-optimization of a poly-generation system for power, heating, cooling, and hydrogen production, J. Therm. Anal. Calorim. 148 (16) (2023) 8195–8221, https://doi.org/10.1007/s10973-022-11793-8, 2023/08/01.

[27] A. Neri, M.A. Butturi, F. Lolli, R. Gamberini, Enhancing waste-to-energy and hydrogen production through urban–industrial symbiosis: a multi-objective optimisation model incorporating a bayesian best-worst method, Smart Cities 7 (2) (2024) 735–757 [Online]. Available: https://www.mdpi.com/2624-6511/7/2/30.

[28] K.Y. Pang, P.Y. Liew, K.S. Woon, W.S. Ho, S.R. Wan Alwi, J.J. Klemeš, Multi-period multi-objective optimisation model for multi-energy urban-industrial symbiosis with heat, cooling, power and hydrogen demands, Energy (Calg.) 262 (2023) 125201, https://doi.org/10.1016/j.energy.2022.125201, 2023/01/01/.

[29] R. Shirmohammadi, A. Aslani, E. Batuecas, R. Ghasempour, L.M. Romeo, F. Petrakopoulou, A comparative life cycle assessment for solar integration in CO2 capture utilized in a downstream urea synthesis plant, J. CO2 Util. 74 (2023) 102534, https://doi.org/10.1016/j.jcou.2023.102534, 2023/08/01/.

[30] A.F. Sotoodeh, F. Ahmadi, Z. Ghaffarpour, M. Ebadollahi, H. Nasrollahi, M. Amidpour, Performance analyses of a waste-to-energy multigeneration system incorporated with thermoelectric generators, Sustain. Energy Technol. Assessments 49 (2022) 101649, https://doi.org/10.1016/j.seta.2021.101649, 2022/02/01/.

[31] F. Petrakopoulou, G. Tsatsaronis, T. Morosuk, Evaluation of a power plant with chemical looping combustion using an advanced exergoeconomic analysis, Sustain. Energy Technol. Assessments 3 (2013) 9–16, https://doi.org/10.1016/j.seta.2013.05.001, 9//.

[32] R. Shirmohammadi, A. Aslani, R. Ghasempour, L.M. Romeo, F. Petrakopoulou, Process design and thermoeconomic evaluation of a CO2 liquefaction process driven by waste exhaust heat recovery for an industrial CO2 capture and utilization plant, J. Therm. Anal. Calorim. 145 (3) (2021) 1585–1597.

[33] M.M. Ismail, I. Dincer, A new renewable energy based integrated gasification system for hydrogen production from plastic wastes, Energy (Calg.) 270 (2023) 126869, https://doi.org/10.1016/j.energy.2023.126869, 2023/05/01/.

[34] I. Uehara, Separation and purification of hydrogen, Energy carriers Convers. Sys. emphas. hydrogenvol 1 (2008) 268–282.

[35] D.-K. Moon, Y. Park, H.-T. Oh, S.-H. Kim, M. Oh, C.-H. Lee, Performance analysis of an eight-layered bed PSA process for H2 recovery from IGCC with pre-combustion carbon capture, Energy Convers. Manag. 156 (2018) 202–214, https://doi.org/10.1016/j.enconman.2017.11.013, 2018/01/15/.

[36] J.-M. Amann, Study of CO2 Capture Processes in Power Plants, École des Mines de Paris, Paris, 2007. PhD thesis.

[37] A.A. Kiss, J. Pragt, H. Vos, G. Bargeman, M. De Groot, Novel efficient process for methanol synthesis by CO2 hydrogenation, Chem. Eng. J. 284 (2016) 260–269.

[38] S.A. Klein, F.J.F.-C.S. Alvarado, Madison, WI, Eng. Equ. solve. 1 (2002).

[39] P. J. Linstrom and W. G. Mallard, Eds. NIST Chemistry Webbook, NIST Standard Reference Database Number 69. Gaithersburg, MD: National Institute of Standards and Technology. [Online]. Available: https://doi.org/10.18434/T4D303.

[40] K.G. Nayar, M.H. Sharqawy, L.D. Banchik, J.H. Lienhard V, Thermophysical properties of seawater: a review and new correlations that include pressure dependence, Desalination 390 (2016) 1–24, https://doi.org/10.1016/j.desal.2016.02.024, 2016/07/15/.

[41] M.H. Sharqawy, J.H. Lienhard, S.M. Zubair, Thermophysical properties of seawater: a review of existing correlations and data, Desalination Water Treat. 16 (1–3) (2010) 354–380.

[42] E. Shayan, V. Zare, I. Mirzaee, On the use of different gasification agents in a biomass fueled SOFC by integrated gasifier: a comparative exergo-economic evaluation and optimization, Energy (Calg.) 171 (2019) 1126–1138, https://doi.org/10.1016/j.energy.2019.01.095, 2019/03/15/.

[43] H. El-Dessouky, I. Alatiqi, H. Ettouney, Process synthesis: the multi-stage flash desalination system, Desalination 115 (2) (1998) 155–179, https://doi.org/10.1016/S0011-9164(98)00035-6, 1998/07/01/.

[44] J.-M. Amann, Study of CO 2 capture processes in power plants, Ecole des Mines de Paris (2007).

[45] H. Nami, F. Mohammadkhani, F. Ranjbar, Utilization of waste heat from GTMHR for hydrogen generation via combination of organic rankine cycles and PEM electrolysis, Energy Convers. Manag. 127 (2016) 589–598, https://doi.org/10.1016/j.enconman.2016.09.043, 2016/11/01/.

[46] P. Ahmadi, I. Dincer, M.A.J.E.C. Rosen, Management, Exergo-Environ. Anal. int. Org. Rankine cycle trigeneration 64 (2012) 447–453.

[47] P. Ahmadi, I. Dincer, Marc A. Rosen, Energy and exergy analyses of hydrogen production via solar-boosted ocean thermal energy conversion and PEM electrolysis 38 (4) (2013) 1795–1805.

[48] S. Ghaem Sigarchian, A. Malmquist, V.J.E. Martin, Design optimization of a small-scale polygeneration energy system in different climate zones in Iran 11 (5) (2018) 1115.

[49] A. Bejan, G. Tsatsaronis, M.J. Moran, Thermal Design and Optimization, John Wiley & Sons, 1995.

[50] R. Shirmohammadi, A. Aslani, R. Ghasempour, L.M. Romeo, F. Petrakopoulou, Techno-economic assessment and optimization of a solar-assisted industrial post-combustion CO2 capture and utilization plant, Energy Rep. 7 (2021) 7390–7404, https://doi.org/10.1016/j.egyr.2021.10.091, 2021/11/01/.

[51] T. Karras, A. Brosowski, D. Thrän, A review on supply costs and prices of residual biomass in techno-economic models for Europe, Sustainability 14 (12) (2022) 7473.

[52] D. Cvetinović, A. Erić, M. Mladenović, J. Buha-Marković, B. Janković, Thermal plasma gasification of sewage sludge: optimisation of operating parameters and economic evaluation, Energy Convers. Manag. 313 (2024) 118639, https://doi.org/10.1016/j.enconman.2024.118639, 2024/08/01/.

[53] M. Wu, et al., Comparative analysis of eight urea-electricity-heat-cooling multi-generation systems: energy, exergy, economic, and environmental perspectives, Energy Convers. Manag. 319 (2024) 118933, https://doi.org/10.1016/j.enconman.2024.118933, 2024/11/01/.

[54] I. Kountouris, L. Langer, R. Bramstoft, M. Münster, D. Keles, Power-to-X in energy hubs: a Danish case study of renewable fuel production, Energy Policy 175 (2023) 113439, https://doi.org/10.1016/j.enpol.2023.113439, 2023/04/01/.

[55] T. Galimova, M. Fasihi, D. Bogdanov, G. Lopez, C. Breyer, Analysis of green e-methanol supply costs: domestic production in Europe versus imports via pipeline and sea shipping, Renew. Energy 241 (2025) 122336, https://doi.org/10.1016/j.renene.2024.122336, 2025/03/01/.

[56] A. Omar, D. Saldivia, Q. Li, R. Barraza, R.A. Taylor, Techno-economic optimization of coupling a cascaded MED system to a CSP-sCO2 power plant, Energy Convers. Manag. 247 (2021) 114725, https://doi.org/10.1016/j.enconman.2021.114725, 2021/11/01/.

[57] C. Serrano-Sanchez, M. Olmeda-Delgado, F. Petrakopoulou, Exergy and economic evaluation of a hybrid power plant coupling coal with solar energy, Appl. Sci. 9 (5) (2019) 850.

[58] L. Pagnini, S. Bracco, F. Delfino, M. de-Simón-Martín, Levelized cost of electricity in renewable energy communities: uncertainty propagation analysis, Appl. Energy 366 (2024) 123278, https://doi.org/10.1016/j.apenergy.2024.123278, 2024/07/15/.

[59] P. Charoensuppanimit, K. Kitsahawong, P. Kim-Lohsoontorn, S. Assabumrungrat, Incorporation of hydrogen by-product from NaOCH3 production for methanol synthesis via CO2 hydrogenation: process analysis and economic evaluation, J. Clean. Prod. 212 (2019) 893–909, https://doi.org/10.1016/j.jclepro.2018.12.010, 2019/03/01/.

[60] G. Schuster, G. Löffler, K. Weigl, H.J. B.t. Hofbauer, Biomass steam Gasification–an extensive parametric modeling study 77 (1) (2001) 71–79.

[61] J.J. Alba, J. Barquín, C. Vereda, E. Moreda, Chapter 4 - integrating the rising variable renewable generation: a Spanish perspective, in: F. Sioshansi (Ed.), Variable Generation, Flexible Demand, Academic Press, 2021, pp. 85–103.

[62] M. Soltanieh, K.M. Azar, M. Saber, Development of a zero emission integrated system for co-production of electricity and methanol through renewable hydrogen and CO2 capture, Int. J. Greenh. Gas Control 7 (2012) 145–152, https://doi.org/10.1016/j.ijggc.2012.01.008, 2012/03/01/.

[63] C. Chen, A. Yang, R. Bañares-Alcántara, Renewable methanol production: understanding the interplay between storage sizing, renewable mix and dispatchable energy price, Adv. Appl. Energy 2 (2021) 100021, https://doi.org/10.1016/j.adapen.2021.100021, 2021/05/26/.

[64] T. Hai, et al., A novel trigeneration model using landfill gas upgrading process and waste heat recovery: application of methanol, desalinated water, and oxygen production, J. Clean. Prod. 393 (2023) 136224, https://doi.org/10.1016/j.jclepro.2023.136224, 2023/03/20/.

[65] K. Farhat, S. Reichelstein, Economic value of flexible hydrogen-based polygeneration energy systems, Appl. Energy 164 (2016) 857–870. https://doi.org/10.1016/j.apenergy.2015.12.008.

[66] I. Tera, S. Zhang, G. Liu, A conceptual hydrogen, heat and power polygeneration system based on biomass gasification, SOFC and waste heat recovery units: energy,

exergy, economic and emergy (4E) assessment, Energy (Calg.) 295 (2024) 131015, https://doi.org/10.1016/j.energy.2024.131015, 2024/05/15/.
[67] B. Wang, X. Yu, J. Chang, R. Huang, Z. Li, H. Wang, Techno-economic analysis and optimization of a novel hybrid solar-wind-bioethanol hydrogen production system via membrane reactor, Energy Convers. Manag. 252 (2022) 115088, https://doi.org/10.1016/j.enconman.2021.115088, 2022/01/15/.
[68] M. Ghema, A. El Fadar, O.B. Achkari, Capacity of waste heat recovery-based polygeneration to achieve sustainable development goals, Sci. Total Environ. 927 (2024) 171983, https://doi.org/10.1016/j.scitotenv.2024.171983, 2024/06/01/.
[69] A. Ray, S. De, Polygeneration using renewable resources: cost optimization using linear programming, Proc. Int. Optim. Sustain. 3 (1) (2019) 115–124, https://doi.org/10.1007/s41660-018-0053-2, 2019/03/01.
[70] S. Shaaban, Performance optimization of an integrated solar combined cycle for the cogeneration of electricity and fresh water, Renew. Energy 227 (2024) 120482, https://doi.org/10.1016/j.renene.2024.120482, 2024/06/01/.
[71] D. Borge-Diez, E. Rosales-Asensio, D. Icaza, E. Açıkkalp, The green hydrogen-water-food nexus: analysis for Spain, Int. J. Hydrogen Energy 77 (2024) 1026–1042, https://doi.org/10.1016/j.ijhydene.2024.06.237.
[72] Z. Michalewicz, M. Schoenauer, Evolutionary algorithms for constrained parameter optimization problems, Evol. Comput. 4 (1) (1996) 1–32, https://doi.org/10.1162/evco.1996.4.1.1.
[73] H. Rostamzadeh, K. Mostoufi, M. Ebadollahi, H. Ghaebi, M. Amidpour, Exergoeconomic optimisation of basic and regenerative triple-evaporator combined power and refrigeration cycles, Int. J. Exergy 26 (1–2) (2018) 186–225.
[74] V. Zare, S.M.S. Mahmoudi, M. Yari, M. Amidpour, Thermoeconomic analysis and optimization of an ammonia–water power/cooling cogeneration cycle, Energy (Calg.) 47 (1) (2012) 271–283, https://doi.org/10.1016/j.energy.2012.09.002, 2012/11/01/.
[75] T. Hai, et al., Enhancing the performance of a novel multigeneration system with electricity, heating, cooling, and freshwater products using genetic algorithm optimization and analysis of energy, exergy, and entransy phenomena, Renew. Energy 209 (2023) 184–205, https://doi.org/10.1016/j.renene.2023.03.088, 2023/06/01/.